Accepted Article

Title: Controlling the Product Platform of Carbon Dioxide Reduction: Adaptive Catalytic Hydrosilylation of CO2 Using a Molecular Cobalt(II) Triazine Complex

Authors: Walter Leitner, Christophe Werlé, Thomas Weyhermüller, Basujit Chatterjee, and Hanna Hinrika Cramer

WILEY-VCH

Controlling the Product Platform of Carbon Dioxide Reduction:

Adaptive Catalytic Hydrosilylation of CO₂ Using a Molecular Cobalt(II) Triazine Complex

Hanna H. Cramer,[a,b] Basujit Chatterjee,[a] Thomas Weyhermüller,[a] Christophe Werlé,[a, c, *] Walter Leitner[a, b, *]

---

[a]   Max Planck Institute for Chemical Energy Conversion, Stiftstr. 34 – 36, 45470 Mülheim an der Ruhr, Germany. Emails: christophe.werle@cec.mpg.de and walter.leitner@cec.mpg.de

[b]   Institut für Technische und Makromolekulare Chemie (ITMC), RWTH Aachen University, Worringer Weg 2, 52074 Aachen, Germany.

[c]   Ruhr University Bochum, Universitätsstr. 150, 44801 Bochum, Germany.

Abstract

The catalytic reduction of carbon dioxide (CO₂) is considered a major pillar of future sustainable energy systems and chemical industries based on renewable energy and raw materials. Typically, catalysts and catalytic systems are transforming CO₂ preferentially or even exclusively to one of the possible reduction levels and are then optimized for this specific product. Here we report a cobalt-based catalytic system that enables the adaptive and highly selective transformation of carbon dioxide individually to either the formic acid, the formaldehyde, or the methanol level, demonstrating the possibility of molecular control over the desired product platform.

1

Introduction

The catalytic reduction of carbon dioxide (CO_2) is considered central to the future of sustainable energy systems and chemical industries based on renewable energy and raw materials.[1] In attempts to "defossilize" the chemical value chain, CO_2 utilization techniques have attracted considerable interest. In particular, the transition metal complex catalyzed reduction of CO_2 can lead to products on the formal oxidation levels of formic acid (HCO_2H),[2] formaldehyde (H_2CO),[3] and methanol (H_3COH),[4] thus providing access to a broad range of valuable chemicals and energy carriers. Research efforts worldwide are focusing on catalytic methods to enable such transformations. Hydro-elementation reactions of CO_2 provide *in-situ* generated intermediates of the three product platforms that can be further hydrolysed or trapped by adding nucleophiles (e.g., amines or alcohols) to generate the corresponding amides or esters, thus creating the opportunity for further functionalization.[5] Catalytic hydrosilylation of CO_2 was used, for example, to activate the notoriously unreactive molecule *en route* to challenging *N*-methylation of amines.[5e, 6]

Typically, catalysts and catalytic systems are amenable to transform CO_2 preferentially or even exclusively to one of the possible reduction levels and are subsequently optimized to provide the corresponding specific product.[2-4] Following these lines, only very few 3d metal complexes are capable of reducing CO_2 beyond the formate level.[3d, 4g, 7] Selected examples of first-row transition metals catalysts for CO_2 hydrosilylation are depicted in Scheme 1.[8] Each of these catalysts leads selectively to one product platform. Interestingly, as reported by Kirchner, Gonsalvi, et al., a manganese complex even allows selective reduction either at the formate level or at the methoxide level, depending on the reaction conditions.[8d]
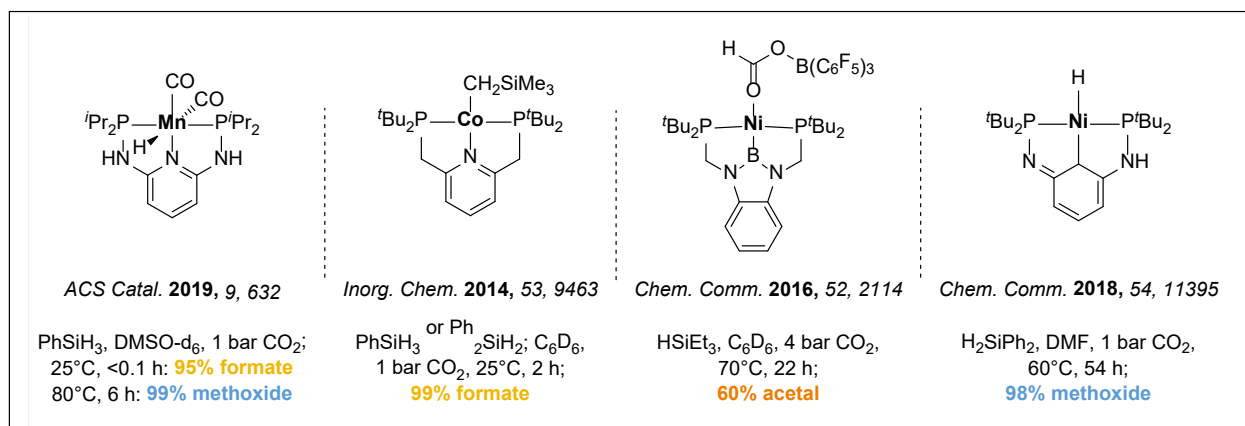
Scheme 1: Selected examples of 3d transition metal catalysts used for CO₂ hydrosilylation.

Alternatively, one might envisage a single catalyst that is comprehensively controlled by fine adjustments of reaction conditions to arrive at any of the different formal oxidation levels of CO$_2$ reduction with high selectivity.[7b, 9] Efforts towards designing such catalytic systems will contribute to an increased understanding of the fundamental requirements needed for the development of adaptive and highly efficient catalytic systems for CO$_2$ reduction.

Here, we present a catalytic system that enables the fully controllable and highly selective transformation of carbon dioxide individually to either the formic acid, the formaldehyde, or to the methanol level, demonstrating the possibility of molecular control over the desired product platform (Scheme 2). The catalyst is based on a coordination compound of the earth-abundant 3d transition metal cobalt, bearing a triazine-core embedded pincer ligand framework.

3
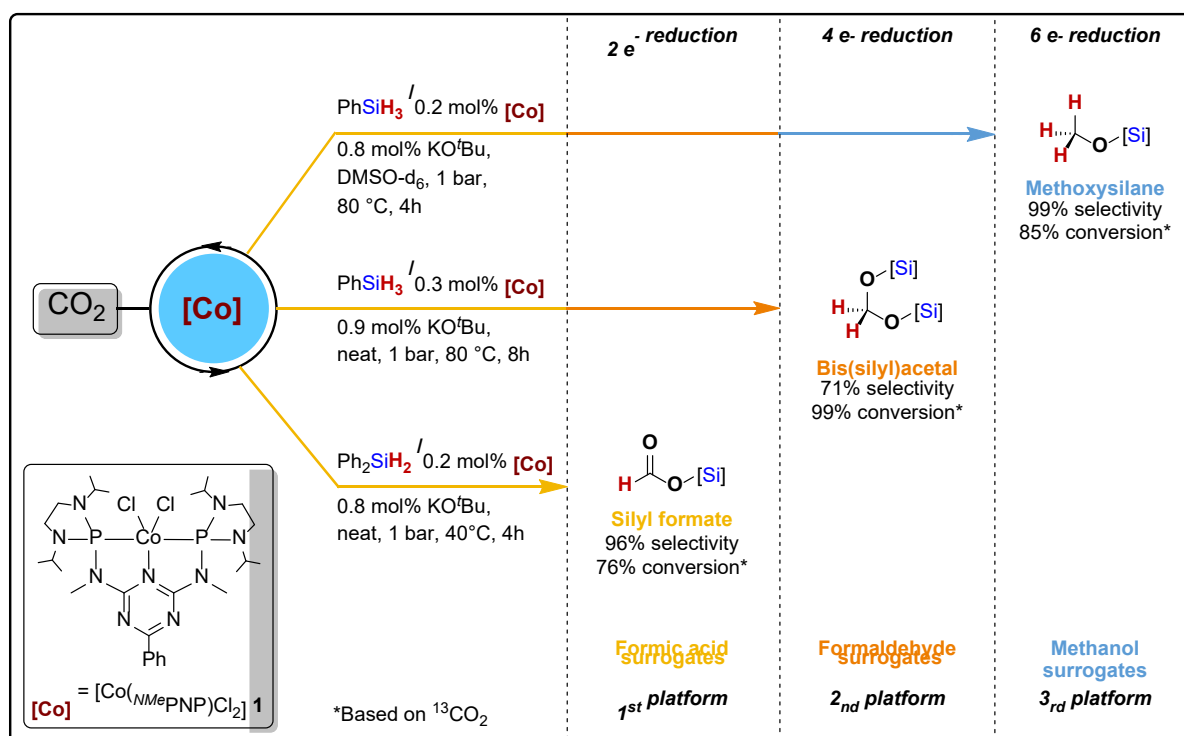
Scheme 2: Controlling the product platform of CO_2 reduction: Adaptive hydrosilylation of CO_2 using the cobalt catalyst **1**.

Results and discussion

Motivated by recent examples of organometallic catalysts of 3d metals comprising PNP pincer type ligands for catalytic CO_2 reduction,[2d, 4a, 10] we set out to explore the catalytic system based on a cobalt complex bearing the triazine ligand **2** ([NMe]PNP) ([NMe]PNP = 2,6-Bis((1,3-diisopropyl-1,3,2-diazaphospholidin)-*N*-methylamino)-4-phenyltriazine). Cobalt has been identified as active 3d metal in formic acid[11] and CO_2 reduction[2e, 3e, 4f, 5d, 7a, 12] previously. Ligand **2** was chosen due to the combination of different electronic effects. The 1,3-diisopropyl-1,3,2-diazaphospholidine moieties are expected to lower significantly the π-back bonding abilities, making the phosphortriamidite groups weaker π-acceptor ligands than phosphines and ultimately leading to higher electron density at the metal center. In contrast, the vertical plane has electron-withdrawing capabilities, *via* the triazine core.[13] Together with the meridional coordination geometry, the ligand defines a well-defined structural and electronic framework around the metal center (Scheme 3).
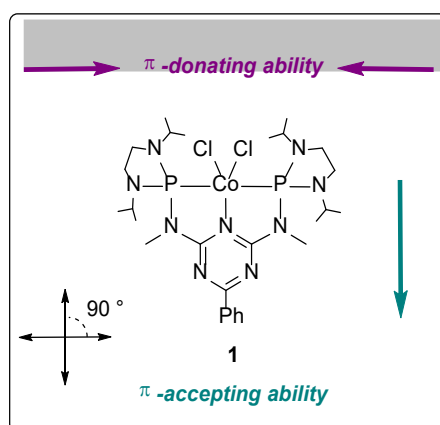
Scheme 3: Electronic considerations in the design of catalyst **1**.

The ligand **2** and the corresponding complex **1** were prepared by following modified reported procedures in the individual steps as described in Scheme 4. The triazine ligand framework was synthesized, starting from commercially available 2,4-dichloro-6-phenyl-1,3,5-triazine **3**. The addition of 2-chloro-1,3-diisopropyl-1,3,2-diazaphospholidine to the lithiated organic backbone in toluene provided the ligand **2**. The subsequent overnight reaction at room temperature of **2** with the $CoCl_2$ in tetrahydrofuran led to the precatalyst [Co([NMe]PNP)Cl$_2$] **1** in 97% yield.
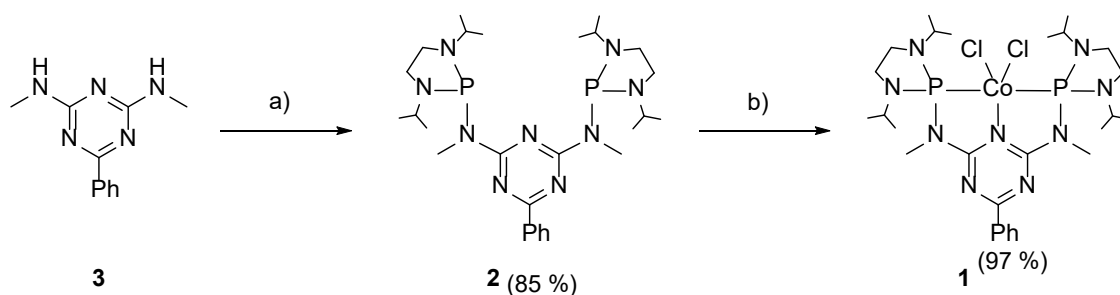
Scheme 4: Reagents and conditions: a) 2-chloro-1,3-diisopropyl-1,3,2-diazaphospholidine, lithium bis(trimethyl-silyl)amide, toluene, 25°C, 16 h; b) CoCl$_2$, THF, 25°C, 12 h.

The formation and structural identity of the products was confirmed by spectroscopic methods in solution and by single crystal X-ray analysis for complex **1**. Single crystals suitable for X-ray diffraction to determine the solid-state molecular structures of **1** were obtained by slow diffusion of *n*-pentane into a concentrated solution of **1** in a mixture of toluene and THF. In Figure 1, the molecular structure of **1** is shown with thermal ellipsoids drawn at the 60% probability level. For clarity reasons, the hydrogen atoms were omitted. Crystallographic data of the complex and a the detailed description of the molecular structure are provided in the supporting information (Table S6). All angles between the *cis*-coordinated donors are close to the ideal value of 90° (83.7 – 94.9°). The apical Co-Cl bond is slightly elongated by 0.17 Å as compared to the Co-Cl bond in the quadratic base. The quadratic pyramidal geometry matches the expectations for a Cobalt(II) complex with a d^7 metal center and is in agreement with structurally related complexes.[14]
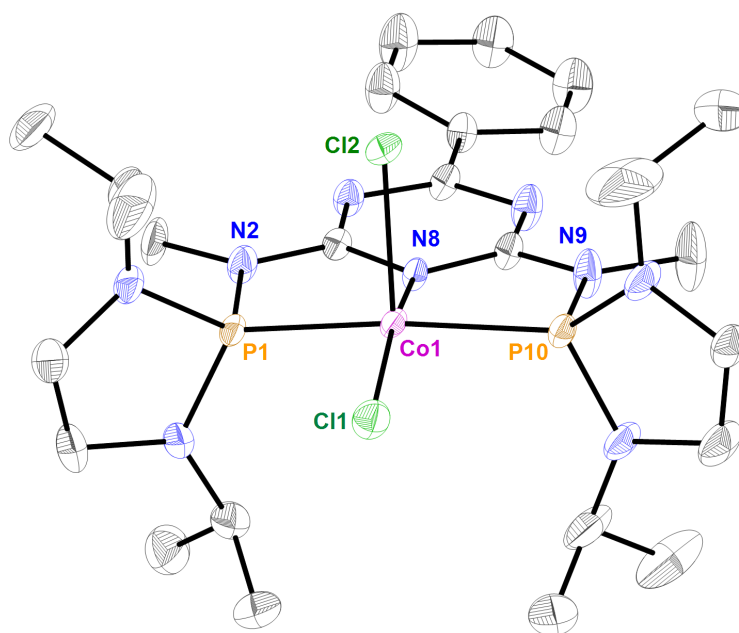
6

Figure 1: Molecular structure of 1. The hydrogen atoms are omitted for clarity. Selected interatomic distances (Å) and angles (°) for **1**: Co1-N8 1.924(3), Co1-P1 2.2079(9), Co1-P10 2.2167(9), P1-N2 1.733(3), P10-N9 1.740(3), Co1-Cl1 2.218(2), Co1-Cl2 2.3885(9), P1-Co1-P10 165.08(4), P1-Co1-N8 83.68(9), P10-Co1-N8 84.79(9)°, N8-Co1-Cl1 164.90(9), Cl2-Co1-N8 87.27(9), Cl2-Co1-P1 94.00(3), Cl2-Co1-P10 94.89(3).

The catalytic activity of the cobalt complex **1** was examined for the hydrosilylation of carbon dioxide with phenylsilane ($PhSiH_3$) at 1 bar applied as a continuous CO_2 stream by using 1 mol% of pre-catalyst and 4 mol% potassium *tert*-butoxide (KO^tBu; relative to the silane) in C_6D_6 at 80 °C for 4 h (Scheme 5). Following previous reports,[7a] conversion and selectivity were determined by quantitative $^{13}C\{^1H\}$ NMR spectroscopy. Silyl formate units correspond to signals at 155-165 ppm, bis(silyl)acetal units to signals at 80-90 ppm, and methoxysilane units to signals at 50-60 ppm.[7a] The cobalt complex **1** converted the CO_2 to silylated products with a total turnover number of 50 for the CO_2, generating the silyl formate, bis(silyl)acetal, and silyl ether units with 51%, 35% and 14% selectivity (Table S1, entry 1). After hydrolysis of the silylated products by adding 0.05 ml water to the reaction mixture and heating at 80°C for 12 h, formic acid and methanol were detected by ^1H NMR spectroscopy, while the trimer of formaldehyde trioxane was observed by GC-MS analysis. No formation of methane was observed in any of these experiments, which is often an undesired side-product in hydro-elementation reactions.[3d, 7a, 9a, 9c, 15]

7
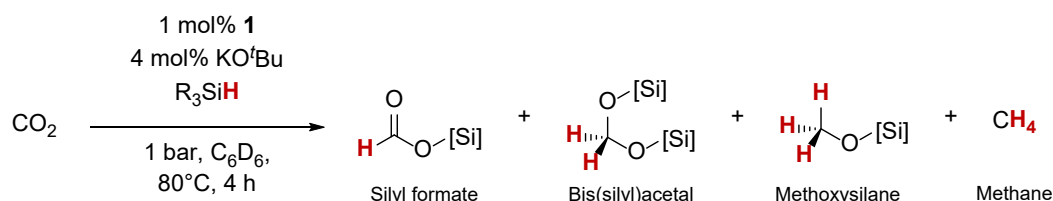
Scheme 5: Screening conditions and possible products for the catalytic hydrosilylation of carbon dioxide using cobalt complex **1**.

Control experiments with 1 mol% $CoCl_2$, with the complex **1** in the absence of KO^{t}Bu, or with KO^{t}Bu alone resulted in no product formation (Table S1, entries 2-3; Table S3 entry 1). Hydrosilylation with complex **1** could be achieved, however, even in the absence of KO^{t}Bu under more rigorous conditions. Treating complex **1** (0.2 mol%) with PhSiH$_3$ for 1 h at room temperature before pressurizing with 40 bar CO_2 and prolonging the reaction time to 21 h resulted in the formation of silyl formates with high selectivity of 91% and a TON of 146 (Table S3, entry 2). The product mixture obtained under the screening conditions revealed a remarkable reactivity of complex **1**, demonstrating that all three reduction levels are accessible with this catalyst. Therefore, we set out to explore the possibility of controlling the reduction process to arrive at individual products selectively.

The influence of the reaction conditions on the reduction pathway was studied systematically using cobalt catalyst **1** with a ratio of 1:4 with potassium *tert*-butoxide as co-catalyst in a closed flask with an initial pressure of 1 bar $^{13}CO_2$ (Table S2). After 4 h at 80°C in C$_6$D$_6$, 97 % conversion of the CO_2 was observed, yielding silyl formate units, bis(silyl)acetal units, and methoxysilane units in 55%, 35%, and 11% selectivity. Decreased catalyst loading of 0.2 mol% **1** and 0.8 mol% KO^{t}Bu resulted in only minor changes of 92% $^{13}CO_2$ conversion and provided 63%, 27% and 10% selectivity for the silyl formate, bis(silyl)acetal and methoxysilane units respectively (Table S2, entries 1-2). Due to the nearly full consumption of $^{13}CO_2$, the turnover numbers of 63 relative to CO_2 conversion and 93 relative to Si-H conversions, respectively, define only a lower limit of the catalyst productivity. These data indicate that the catalyst is able to convert CO_2 even under very low partial pressures.

8

The catalyst loading of 0.2 mol% **1** and 0.8 mol% KO^{t}Bu with 2.5 mmol silane was set as standard conditions in the subsequent studies. In agreement with previous reports, the choice of the solvent strongly influenced the selectivity of the reaction (Table S2, entries 3-6).[16] As displayed in Figure 2, the conversion of $^{13}CO_2$ was further increased to 94 % under neat conditions while the selectivity changed from the silyl formats as the main product (63% selectivity in C_6D_6) to the bis(silyl)acetals (53% selectivity, neat). Using DMSO-d$_6$ as the solvent, the reduction reached almost exclusively to the methanol level forming the methoxysilane units with excellent selectivity of more than 99% with a $^{13}CO_2$ conversion of 85%. Other polar solvents such as acetonitrile or THF, proved less effective. Conversion of $^{13}CO_2$ was still significant when the weaker reductant diphenylsilane (Ph$_2$SiH$_2$) was used as the silylating agent under the standard conditions (Table S2, entries 7-8). The reduction was steered towards the formate level, with the preferential formation of silyl formates in high selectivity. 79% selectivity and 70% $^{13}CO_2$ conversion were observed under neat conditions, 75% selectivity and 57% $^{13}CO_2$ conversion in C_6D_6.
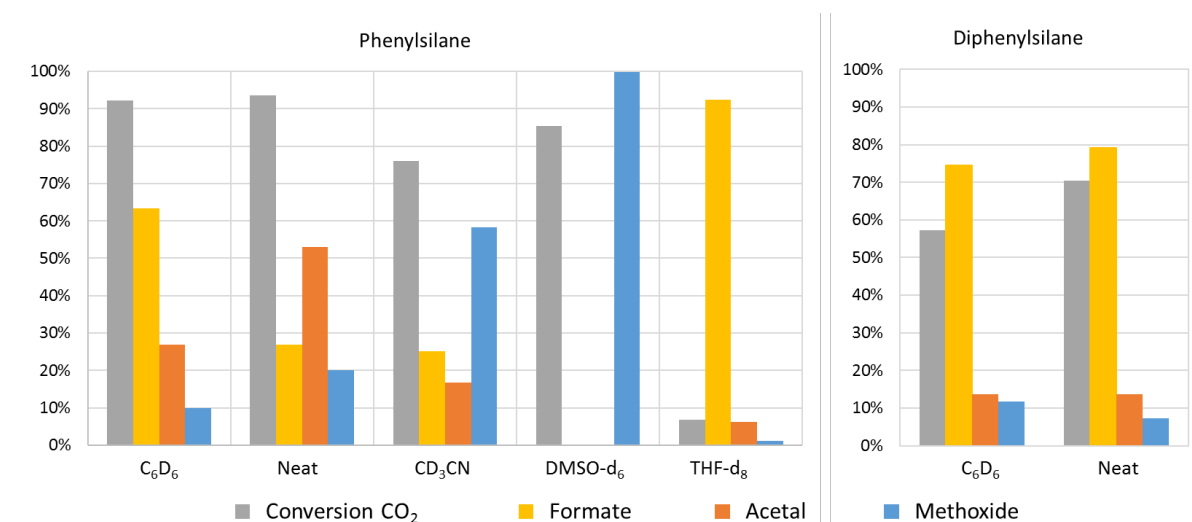

Figure 2: Influence of the solvent and the silane for the hydrosilylation of carbon dioxide. 1 bar $^{13}CO_2$, 0.2 % catalyst loading, 0.8 % base loading, 80°C, 4 h

The influence of temperature was evaluated under neat conditions under 1 bar of $^{13}CO_2$ (Table S2, entries 9-12). As shown in Figure 3, the high CO_2 conversion of 90% - 94% was achieved in a range from room temperature to 80°C. At higher temperatures, the conversion decreased down to only 47% at 120°C. This may be due to catalyst deactivation or non-productive silane dehydrogenation at higher temperatures. A clear trend for the product

9

formation of CO_2 reduction can be observed. The formate level is strongly favored at low temperatures leading to maximum selectivity of 79% for the silyl formates at room temperature. The reduction beyond the formate level becomes increasingly pronounced at higher temperatures, with a strong preference for the 53% selective acetal formation at 80°C. With the formaldehyde platform being the most difficult to reach reduction level, the 53% selectivity obtained in this parameter study is already quite remarkable.
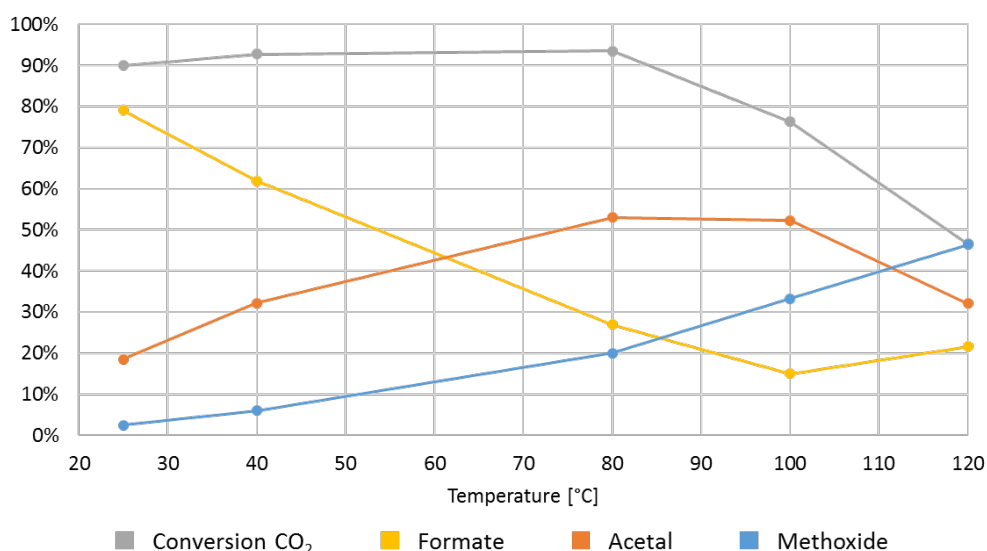

Figure 3: Influence of the temperature on the hydrosilylation of carbon dioxide with complex **1** and phenylsilane. 1 bar $^{13}CO_2$, 0.2 mol% catalyst loading, 0.8 mol% base loading, neat, 4 h.

The CO_2 pressure had only a small effect on the total CO_2 consumption but strongly influenced the selectivity. As shown in Figure 4, the selectivity towards the silyl formates increases from 53% at 1 bar with a constant gas flow to 83% at 40 bar in a closed vessel. The turnover numbers (relative to the product formation) for reduction to the formate level correspond to turnover numbers of 355 at 1 bar and 468 and 508 at 20 and 40 bar (Table S1, entry 4; Table S3, entries 3-4).
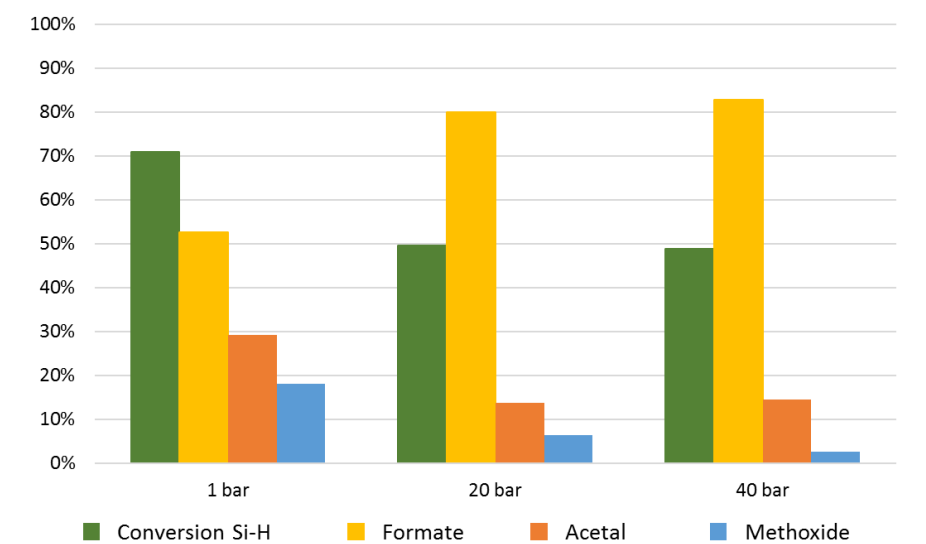
10

Figure 4: Influence of the CO_2 pressure on the hydrosilylation of carbon dioxide using catalyst **1**. Phenylsilane, 0.2 % catalyst loading, 0.8 % base loading, neat, 80°C, 4 h.

Table 1 summarizes the influence of the control parameters on product formation. In a first approximation, they correspond with the relative kinetic challenge for the reduction levels.[1f, 5f, 15d] Hydride transfer to reduce CO_2 to formate has a relatively low barrier, making this product accessible at low temperatures and a low Si-H/CO_2 ratio corresponding to a weaker reductant and higher CO_2 pressures. Highly polar aprotic solvents, as represented by DMSO, are beneficial for the further hydride transfer.[16] Additionally, low CO_2 pressures (high Si-H/CO_2 ratio) and higher temperatures facilitate the reduction. Most challenging is the control on the formaldehyde level, which is kinetically disfavored relative to both the formation as well as the over-reduction.

Table 1: Control parameters for selective product formation

Reduction level / Parameter	Formic acid [Si]-O_2CH	Formaldehyde [Si]-OCH_2O-[Si]	Methanol [Si]-OCH_3
Solvent	Broad range	Neat	Dipolar aprotic
Silane	Broad range	$PhSiH_3$	$PhSiH_3$
Temperature	Low	Medium	High
CO_2 supply	High pressure or continuous	Low pressure, static	Low pressure, static or continuous
Si-H/CO_2	Low	Medium	High

11

While the exact nature of the catalytic active species remains at present elusive, the deduced trends are consistent with hydride transfer to the C=O units of the individual products/substrates as the major mechanistic control factor. Thus, rational optimization to maximize the yields for the individual products becomes possible, as outlined below and summarized in Figure 5.

To reach the **formate level** in high yields, a low Si-H:CO_2 ratio with the use of diphenylsilane as silylating agent in the absence of solvent was set as primary conditions (2.5 mmol silane, 0.2 mol% Co, **1**:KO^{t}Bu 1:4). Under 40 bar CO_2 pressure, a catalyst solution based on complex **1** produced 1.2 mmol silyl formate units in 93% selectivity in 4 h. This corresponds to a conversion of Si-H units of 26% and TON relative to the Si-H transfer of 264. Carrying out the reaction at 1 bar $^{13}CO_2$ and 40°C under neat conditions for 4 h, 76% of the $^{13}CO_2$ was converted to silyl formate units with high selectivity of 96% (Figure 5, column 1 and 3).

Highly selective reduction to the **methanol level** was achieved in DMSO-d$_6$ at 80°C under a constant flow of CO_2 at 1 bar for 4 h with PhSiH$_3$ (2.5 mmol silane, 0.2 mol% Co, **1**:KO^{t}Bu 1:4). The methoxysilane units were formed with 99% selectivity at 68% conversion of silane in quantities corresponding to a TON of 277 (Figure 5, column 5). Interestingly, increasing the pressure to 40 bar under otherwise identical conditions led to a drastic change in selectivity towards the formate units with excellent selectivity of 98% and a turnover number of 262 (Figure 5, column 2). This suggests that for hydrosilylation in DMSO-d$_6$, the Si-H:CO_2 ratio is the predominant control parameter making this reaction highly pressure tunable under these conditions.[9c]

For the most challenging **formaldehyde level**, the selectivity was optimized by compromising between formation and over-reduction. In the optimization sequence, the best selectivity of 53% and a TON of 56 were already obtained in the initially used solvent-free standard conditions (2.5 mmol silane, 0.2 mol% Co, **1**:KO^{t}Bu 1:4, 80°C, 1 bar, 4 h) and with phenylsilane as the silylating agent. Increasing the **1**:KO^{t}Bu ratio to 1:7 under otherwise identical conditions gave a similar selectivity of 62% and a TON of 40, although the CO_2 conversion was lower (82% compared to 94%). The highest selectivity of bis(silyl)acetals with 71% was achieved under neat conditions and a 1 bar $^{13}CO_2$ by slightly modifying the standard conditions to 0.3% **1**,

12

0.9% potassium *tert*-butoxide and 8 h reaction time (Figure 5, column 4). While reduction of the formate was nearly complete (6%), the over reduction to the methoxysilyl units could not be fully suppressed and accounted for 23% of products.
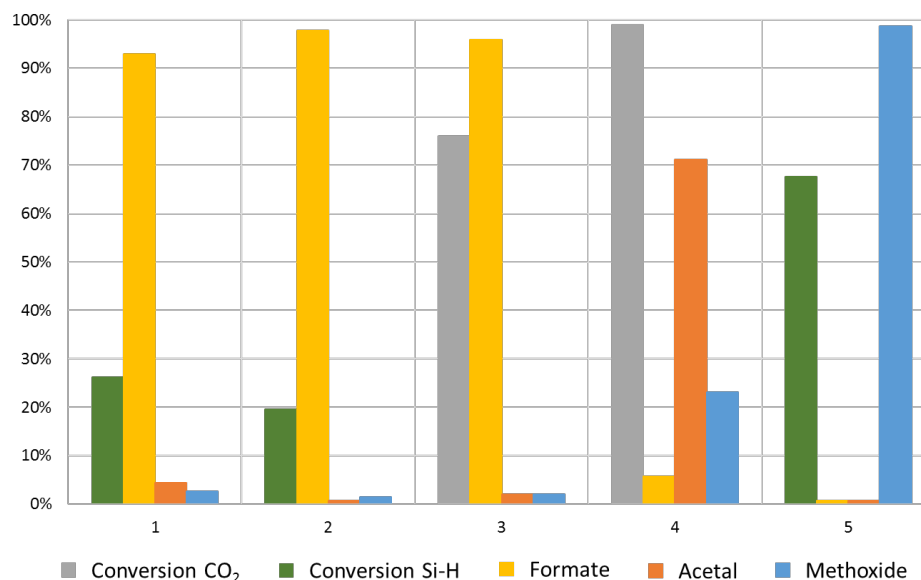

Figure 5: Conversion and product selectivity under optimized reaction conditions for the hydrosilylation of carbon dioxide. Column 1: 0.2% **1**, 0.8 % KO^{t}Bu, H$_2$SiPh$_2$, 40 bar, neat, 80°C, 4 h; Column 2: 0.2% **1**, 0.8 % KO^{t}Bu, H$_3$SiPh, 40 bar, DMSO-d$_6$, 80°C, 4 h; Column 3: 0.2% **1**, 0.8 % KO^{t}Bu, 1 bar ^{13}CO$_2$, neat, H$_2$SiPh$_2$, 40°C, 4 h; Column 4: 0.3 % **1**, 0.9 % KO^{t}Bu, H$_3$SiPh, 1 bar ^{13}CO$_2$, neat, 80°C, 8 h; Column 5: 0.2 % **1**, 0.8 % KO^{t}Bu, H$_3$SiPh, 1 bar (continuous gas stream), DMSO-d$_6$, 80°C, 4 h.

13

Conclusion

In conclusion, we have developed an efficient catalyst, which demonstrates remarkable selectivity in CO_2 reduction towards attaining individually the product platforms of formic acid (HCO_2H), formaldehyde (H_2CO), and methanol (H_3COH). The cobalt-based catalyst bearing a PNP pincer-type triazine ligand can operate at low catalyst loadings (0.2 mol%), short reaction times (4 h), and moderate temperatures (r.t. to 80°C) to convert CO_2 even at ambient pressures. The formate level can be adjusted at 96% selectivity via hydrosilylation using diphenylsilane under solvent-free conditions at 40°C for 4 h, while the methanol level is reachable in DMSO at 80°C for 4 h in 99% selectivity by using phenylsilane. The formaldehyde level is accessible in 71% selectivity by using phenylsilane under neat conditions for 8 h at 80°C. These results demonstrate the adaptivity of the catalytic system under varying reaction conditions for the development of catalytic protocols to selectively access different reduction levels of CO_2 Further studies to elucidate the nature of the active species are currently underway to fully comprehend the underlying control mechanisms on a molecular basis. Meanwhile, extending the concept of multi-level CO_2 reduction to other reducing agents, including hydrogen or electrons and protons, seems highly attractive.

Supplementary Information is linked to the online version of the paper at anie_xxxxxxxxx_sm_miscellaneous_information.pdf

Acknowledgments

Literature

[1] a) E. A. Quadrelli, G. Centi, J. L. Duplan, S. Perathoner, *ChemSusChem* **2011**, *4*, 1194-1215; b) P. Markewitz, W. Kuckshinrichs, W. Leitner, J. Linssen, P. Zapp, R. Bongartz, A. Schreiber, T. E. Müller, *Energy Environ. Sci.* **2012**, *5*, 7281-7305; c) J. Schneider, H. Jia, J. T. Muckerman, E. Fujita, *Chem. Soc. Rev.* **2012**, *41*, 2036-2051; d) M. Aresta, A. Dibenedetto, A. Angelini, *Chem. Rev.* **2014**, *114*, 1709-1742; e) Q. Liu, L. Wu, R. Jackstell, M. Beller, *Nat. Commun.* **2015**, *6*, 5933; f) J. Klankermayer, S. Wesselbaum, K. Beydoun, W. Leitner, *Angew. Chem. Int. Ed.* **2016**, *55*, 7296-7343; g) J. Artz, T. E. Müller, K. Thenert, J. Kleinekorte, R. Meys, A. Sternberg, A. Bardow, W. Leitner, *Chem. Rev.* **2018**, *118*, 434-504.

[2] a) W. Leitner, *Angew. Chem. Int. Ed.* **1995**, *34*, 2207-2221; b) R. Tanaka, M. Yamashita, K. Nozaki, *J. Am. Chem. Soc.* **2009**, *131*, 14168–14169; c) C. Federsel, A. Boddien, R. Jackstell, R. Jennerjahn, P. J. Dyson, R. Scopelliti, G. Laurenczy, M. Beller, *Angew. Chem. Int. Ed.* **2010**, *49*, 9777-9780; d) R. Langer, Y. Diskin-Posner, G. Leitus, L. J. Shimon, Y. Ben-David, D. Milstein, *Angew. Chem. Int. Ed.* **2011**, *50*, 9948-9952; e) M. S. Jeletic, M. T. Mock, A. M. Appel, J. C. Linehan, *J. Am. Chem. Soc.* **2013**, *135*, 11533-11536; f) C. A. Huff, M. S. Sanford, *ACS Catal.* **2013**, *3*, 2412-2416; g) S. Moret, P. J. Dyson, G. Laurenczy, *Nat. Commun.* **2014**, *5*, 4017; h) G. A. Filonenko, R. van Putten, E. N. Schulpen, E. J. M. Hensen, E. A. Pidko, *ChemCatChem* **2014**, *6*, 1526-1530; i) Y. Zhang, A. D. MacIntosh, J. L. Wong, E. A. Bielinski, P. G. Williard, B. Q. Mercado, N. Hazari, W. H. Bernskoetter, *Chem. Sci.* **2015**, *6*, 4291-4299; j) J. Klankermayer, S. Wesselbaum, K. Beydoun, W. Leitner, *Angew. Chem. Int. Ed.* **2016**, *55*, 7296-7343.

[3] a) S. Bontemps, L. Vendier, S. Sabo-Etienne, *Angew. Chem. Int. Ed.* **2012**, *51*, 1671-1674; b) S. Bontemps, L. Vendier, S. Sabo-Etienne, *J. Am. Chem. Soc.* **2014**, *136*, 4419-4425; c) P. Rios, N. Curado, J. Lopez-Serrano, A. Rodriguez, *Chem. Commun. (Camb.)* **2016**, *52*, 2114-2117; d) M. Rauch, G. Parkin, *J. Am. Chem. Soc.* **2017**, *139*, 18162-18165; e) B. G. Schieweck, J. Klankermayer, *Angew. Chem. Int. Ed.* **2017**, *56*, 10854-10857; f) N. Del Rio, M. Lopez-Reyes, A. Baceiredo, N. Saffon-Merceron, D. Lutters, T. Müller, T. Kato, *Angew. Chem. Int. Ed.* **2017**, *56*, 1365-1370; g) M. Rauch, Z. Strater, G. Parkin, *J. Am. Chem. Soc.* **2019**, *141*, 17754-17762.

[4] a) S. Chakraborty, J. Zhang, J. A. Krause, H. Guan, *J. Am. Chem. Soc.* **2010**, *132*, 8872-8873; b) G. A. Olah, A. Goeppert, G. K. S. Prakash, *Beyond Oil and Gas: The Methanol Economy*, Wiley-VCH, **2011**; c) C. A. Huff, M. S. Sanford, *J. Am. Chem. Soc.* **2011**, *133*, 18122-18125; d) S. Wesselbaum, T. Vom Stein, J. Klankermayer, W. Leitner, *Angew. Chem. Int. Ed.* **2012**, *51*, 7499-7502; e) N. M. Rezayee, C. A. Huff, M. S. Sanford, *J. Am. Chem. Soc.* **2015**, *137*, 1028-1031; f) J. Schneidewind, R. Adam, W. Baumann, R. Jackstell, M. Beller, *Angew. Chem. Int. Ed.* **2017**, *56*, 1890-1893; g) C. Erken, A. Kaithal, S. Sen, T. Weyhermüller, M. Hölscher, C. Werlé, W. Leitner, *Nat. Commun.* **2018**, *9*, 4521; h) W.-Y. Chu, Z. Culakova, B. T. Wang, K. I. Goldberg, *ACS Catal.* **2019**, *9*, 9317-9326.

[5]   a) O. Jacquet, C. Das Neves Gomes, M. Ephritikhine, T. Cantat, *J. Am. Chem. Soc.* **2012**, *134*, 2934-2937; b) L. González-Sebastián, M. Flores-Alamo, J. J. García, *Organometallics* **2013**, *32*, 7186-7194; c) O. Jacquet, C. Das Neves Gomes, M. Ephritikhine, T. Cantat, *ChemCatChem* **2013**, *5*, 117-120; d) P. Daw, S. Chakraborty, G. Leitus, Y. Diskin-Posner, Y. Ben-David, D. Milstein, *ACS Catal.* **2017**, *7*, 2500-2504; e) D. S. Morris, C. Weetman, J. T. C. Wennmacher, M. Cokoja, M. Drees, F. E. Kühn, J. B. Love, *Catal. Sci. Technol.* **2017**, *7*, 2838-2845; f) Y. Zhang, T. Zhang, S. Das, *Green Chem.* **2020**, *22*, 1800-1820.

[6]   a) Y. Li, X. Fang, K. Junge, M. Beller, *Angew. Chem. Int. Ed.* **2013**, *52*, 9568-9571; b) C. Darcel, J.-B. Sortais, D. Wei, A. Bruneau-Voisine, in *Non-Noble Metal Catalysis*, **2018**, pp. 241-264.

[7]   a) M. L. Scheuermann, S. P. Semproni, I. Pappas, P. J. Chirik, *Inorg. Chem.* **2014**, *53*, 9463-9465; b) F. Bertini, M. Glatz, B. Stöger, M. Peruzzini, L. F. Veiros, K. Kirchner, L. Gonsalvi, *ACS Catal.* **2018**, *9*, 632-639.

[8]   a) M. L. Scheuermann, S. P. Semproni, I. Pappas, P. J. Chirik, *Inorg. Chem.* **2014**, *53*, 9463-9465; b) P. Ríos, N. Curado, J. López-Serrano, A. Rodríguez, *Chem. Comm.* **2016**, *52*, 2114-2117; c) H. Li, T. P. Gonçalves, Q. Zhao, D. Gong, Z. Lai, Z. Wang, J. Zheng, K.-W. Huang, *Chem. Comm.* **2018**, *54*, 11395-11398; d) F. Bertini, M. Glatz, B. Stöger, M. Peruzzini, L. F. Veiros, K. Kirchner, L. Gonsalvi, *ACS Catal.* **2019**, *9*, 632-639.

[9]   a) T. T. Metsänen, M. Oestreich, *Organometallics* **2014**, *34*, 543-546; b) M. R. Espinosa, D. J. Charboneau, A. Garcia de Oliveira, N. Hazari, *ACS Catal.* **2018**, *9*, 301-314; c) J. Guzmán, P. García-Orduña, V. Polo, F. J. Lahoz, L. A. Oro, F. J. Fernández-Alvarez, *Catal. Sci. Technol.* **2019**, *9*, 2858-2867.

[10]   A. Kumar, P. Daw, N. A. Espinosa-Jalapa, G. Leitus, L. J. W. Shimon, Y. Ben-David, D. Milstein, *Dalton Trans.* **2019**, *48*, 14580-14584.

[11]   T. J. Korstanje, J. Ivar van der Vlugt, C. J. Elsevier, B. de Bruin, *Science* **2015**, *350*, 298.

[12]   a) C. Federsel, C. Ziebart, R. Jackstell, W. Baumann, M. Beller, *Chem.: Eur. J.* **2012**, *18*, 72-75; b) M. S. Jeletic, M. L. Helm, E. B. Hulley, M. T. Mock, A. M. Appel, J. C. Linehan, *ACS Catal.* **2014**, *4*, 3755-3762.

[13]   a) M. Joost, L. Estevez, S. Mallet-Ladeira, K. Miqueu, A. Amgoune, D. Bourissou, *Angew. Chem. Int. Ed.* **2014**, *53*, 14512-14516; b) G. Bistoni, S. Rampino, N. Scafuri, G. Ciancaleoni, D. Zuccaccia, L. Belpassi, F. Tarantelli, *Chem. Sci.* **2016**, *7*, 1174-1184.

[14]   S. Rösler, J. Obenauf, R. Kempe, *J. Am. Chem. Soc.* **2015**, *137*, 7998-8001.

[15]   a) T. Matsuo, H. Kawaguchi, *J. Am. Chem. Soc.* **2006**, *128*, 12362-12363; b) S. J. Mitton, L. Turculet, *Chem.: Eur. J.* **2012**, *18*, 15258-15262; c) S. Park, D. Bezier, M. Brookhart, *J. Am. Chem. Soc.* **2012**, *134*, 11404-11407; d) F. J. Fernández-Alvarez, A. M. Aitani, L. A. Oro, *Catal. Sci. Technol.* **2014**, *4*, 611-624; e) A. Julián, E. A. Jaseer, K. Garcés, F. J. Fernández-Alvarez, P. García-Orduña, F. J. Lahoz, L. A. Oro, *Catal. Sci. Technol.* **2016**,

16

6, 4410-4417; f) F. J. Fernández-Alvarez, L. A. Oro, *ChemCatChem* **2018**, *10*, 4783-4796; g) J. Chen, M. McGraw, E. Y. Chen, *ChemSusChem* **2019**, *12*, 4543-4569.

[16]   H. Lv, Q. Xing, C. Yue, Z. Lei, F. Li, *Chem. Commun. (Camb.)* **2016**, *52*, 6545-6548.

Accepted Manuscript